12-Crown-4–Ether and Tri(ethylene glycol) Dimethyl–Ether Plasma-Coated Stainless Steel Surfaces and Their Ability to Reduce Bacterial Biofilm Deposition

AGNES R. DENES,[1] EILEEN B. SOMERS,[1] AMY C. L. WONG,[1] FERENCZ DENES[2]

[1] Food Research Institute, University of Wisconsin–Madison, 1925 Willow Drive, Madison, Wisconsin 53706

[2] Center for Plasma-Aided Manufacturing, University of Wisconsin–Madison, 1410 Engineering Drive, Madison, Wisconsin 53706

Received 13 July 2000; accepted 12 November 2000

ABSTRACT: It has been demonstrated that surfaces coated with poly(ethylene glycol) (PEG) are capable of reducing protein adsorption, bacterial attachment, and biofilm formation. In this communication cold-plasma–enhanced processes were employed for the deposition of PEG-like structures onto stainless steel surfaces. Stainless steel samples were coated under 1,4,7,10-tetraoxacyclododecane (12-crown-4)–ether and tri(ethylene glycol) dimethyl ether (triglyme)–radio frequency (RF)–plasma conditions. The chemistry and characteristics of plasma-coated samples and biofilms were investigated using electron spectroscopy for chemical analysis (ESCA), atomic force microscopy (AFM), and water contact angle analysis. ESCA analysis indicated that the plasma modification resulted in the deposition of PEG-like structures, built up mainly of $–CH_2—CH_2—O–$ linkages. Plasma-coated stainless steel surfaces were more hydrophilic and had lower surface roughness values compared to those of unmodified substrates. Compared to the unmodified surfaces, they not only significantly reduced bacterial attachment and biofilm formation in the presence of a mixed culture of S*almonella typhimurium, Staphylococcus epidermidis,* and *Pseudomonas fluorescens* but also influenced the chemical characteristics of the biofilm. Thus, plasma deposition of PEG-like structures will be of use to the food-processing and medical industries searching for new technologies to reduce bacterial contamination. © 2001 John Wiley & Sons, Inc. J Appl Polym Sci 81: 3425–3438, 2001

Key words: bacterial attachment; biofilm formation; cold-plasma–induced surface modification; PEG-like structures; surface chemistry

INTRODUCTION

Attachment of bacteria to surfaces can result in the formation of biofilms that create economic and health problems in many environments, including the food and medical industries. Biofilms can be broadly defined as bacterial cells attached to a surface, which are frequently embedded in a polymer matrix of microbial origin. Biofilms formed on equipment surfaces, conveyor belts, floors, drains, and packaging materials in food-processing environments are a potential source for food contamination and can result in transmission of food-borne diseases and reduced shelf life of food products. Biofilms that develop on biomedical devices such as prostheses, catheters, and implants

Correspondence to: A. Wong.

Journal of Applied Polymer Science, Vol. 81, 3425–3438 (2001)

can result in infections and cause health problems. Development of new technologies to prevent or at least attenuate biofilm formation, as described in this study, is highly desirable.

The interaction of biological materials with various surfaces is controlled by their physical and chemical characteristics (e.g., surface charge, hydrophobicity, topography). It is recognized that a first step in biofilm formation is the adsorption of macromolecules such as proteins followed by attachment of bacteria.[1] Surfaces that can prevent attachment of proteins and bacteria consequently will inhibit biofilm formation. Poly(ethylene glycol) (PEG) has been explored as a potential antifouling material.[2–4] Although the mechanisms for the antifouling behavior of PEG structures are not yet fully understood, some of the properties of these polymers may account for the low protein-adsorption characteristics. PEG chains are highly flexible and can cause an intense entropic repulsion of protein molecules, which is attributed to the reduced degrees of conformational freedom of protein macromolecular chains.[3,5] PEG is highly water soluble, and as a result of hydrogen bonds created between the oxygen atoms of PEG and water molecules, a water-molecule–cluster shield is generated around the PEG macromolecular chains. Surfaces coated with PEG layers were found to resist bacterial attachment.[6] Self-assembled monolayers formed by the adsorption of ω-substituted alkanethiols on transparent gold films were evaluated for the attachment of *Staphylococcus epidermidis* and *Deleya marina*.[7] It was shown that C-substituted hexa(ethylene glycol) groups were uniformly resistant to bacterial attachment (>99.7% reduction for both organisms), whereas C-substituted methyl, carboxylic acid, and fluorocarbon groups exhibited very different bacterial attachment responses.

PEG-coated surfaces are usually produced using classical wet chemistry techniques, including direct adsorption and covalently binding (e.g., grafting) of PEG molecules via a predeposited functional polymeric structure, using virgin PEG or its modified structures.[6,8,9] However, most of these techniques involve multistep processes and often require the use of environmentally harmful chemical reagents.

Cold-plasma technologies open up new and more efficient routes for the synthesis and deposition of PEG-type structures. It has been demonstrated that by selecting the proper plasma parameters the plasma-mediated reaction mechanisms can be controlled. This very efficient and dry technology, originally considered mainly for passivation coatings, currently is focused on applications where the surface structures critically control device performances (e.g., sensors, dielectric films, etc.).[10–12]

Plasma-enhanced coatings have been used for inhibiting protein adhesion. It was shown that protein adsorption was diminished significantly when poly(2-methacryloyloxyethyl phosphorylcholine) was grafted onto argon–plasma-activated silicone rubber substrate surfaces.[13] It was also found that hydrophilic surfaces resulting from allyl alcohol– and allyl amine–plasma-treated poly(ethylene terephthalate) (PET) surfaces retained slightly lower protein quantities compared to that of hydrophobic surfaces generated under perfluorohexene– and hexamethylsiloxane–plasma conditions. The extent of fibrinogen adsorption on these surfaces was closely related to the presence of specific plasma-generated functionalities (–OH; $–NH_2$; $–CF_3$).[14]

Because of the diversity of plasma-reactor characteristics (e.g., reactor geometry, electrode configuration, geometrical location of the substrates) and the plasma parameters (e.g., power, pressure, nature of plasma gases) employed, the resulting surface characteristics are often difficult to compare. Accordingly, some of the approaches designed for the plasma-enhanced deposition of antifouling layers are oriented exclusively toward the generation of PEG-like structures by using volatile derivatives of oligo-PEG as starting components. It was previously demonstrated, for instance, that oligo(glyme) [e.g., tetra(ethylene glycol) dimethyl ether (TEGDME)]–plasma discharges resulted in the deposition of PEG-like macromolecular networks,[15,16] and that the substrates coated under mild TEGDME–plasma conditions (pulsed plasma, low power settings) exhibited extremely low protein adsorption and enhanced the attachment of human blood platelets and bovine aortic endothelial cells.[17] High-resolution C1s electron spectroscopy for chemical analysis (ESCA) of TEGDME and tri(ethylene glycol) dimethyl ether (triglyme)–plasma-coated samples indicated that the chemical structure (in which the C—O bond is the major component) and atomic composition of the deposited films were similar to the structure and atomic composition of PEG.[17,18]

Considerably less work has been done in the area of plasma modification of surfaces directed toward the prevention of bacterial attachment and biofilm formation. Nonetheless, it was found that dimeth-

ylaminoethylmethacrylate– and acrylic acid–plasma treatments of selected medical sutures significantly reduced the attachment of coagulase-positive staphylococci, *Streptococcus pyogenes,* and *Escherichia coli.*[19] It was demonstrated that attachment of hydrophobic bacteria was decreased by increasing the hydrophilicity of the substrate surfaces.[20] However, significantly different results were obtained with different bacterial species. Coagulase-positive staphylococci, for example, showed very low attachment levels on plasma-generated hydrophobic and hydrophilic surfaces, whereas *S. epidermidis* exhibited enhanced adhesion to hydroxyethylmethacrylate– and oxygen–plasma-exposed polystyrene film surfaces. Radio frequency (RF) glow discharge plasma was used to deposit triglyme on polyetherurethane (PEU) surfaces.[21] Attachment of *Pseudomonas aeruginosa* was reduced by 99.3% and biofilm formation by 93.5% on the coated PEU when compared to the untreated surfaces.

The present contribution reports on the use of 12-crown-4–ether and triglyme RF–plasma environments for the synthesis of PEG-like structures and the evaluation of their efficacy to reduce bacterial attachment and biofilm formation. Thin-layer macromolecular structures were deposited under continuous wave (CW) oxygen–plasma and 12-crown-4 and triglyme pulsed plasma (PP) conditions onto stainless steel (SS), a material commonly used in food processing equipment and biomedical devices. PP conditions were selected to diminish molecular fragmentation of 12-crown-4 and triglyme. With properly selected duty cycles the extent of plasma-induced dissociation reactions could be controlled. Formation of macromolecular structures occurs through the recombination of less-fragmented species with the active sites of plasma-exposed nascent surfaces.[22–25] During the formation and deposition of PEG-like structures a balance should be achieved between fragmentation/dehydrogenation and the synthesis of PEG chains. The plasma-deposited macromolecular networks must retain a significant amount of $–CH_2—CH_2—O–$ repeating units to exhibit antifouling characteristics, and at the same time should have a crosslinked nature to overcome the water-solubility problem.

The surface chemistry and characteristics of unmodified and plasma-modified SS were investigated using survey and high-resolution ESCA, atomic force microscopy (AFM), and contact angle evaluations. The ability of the plasma-modified samples to reduce bacterial attachment and biofilm formation was assessed.

EXPERIMENTAL

Materials

Stainless steel sheets (type 304, No. 4 finish, 24-gauge) were obtained from Temperature Systems (Madison, WI). Chips of 1-cm^2 surface area were cut and washed in a hot alkaline detergent (Micro; International Products, Trenton, NJ) for 30 min, rinsed five times in distilled water, and air-dried. Oxygen was obtained from Liquid Carbonic (Brookfield, WI), and 12-crown-4 and triglyme were purchased from Aldrich Chemical (Milwaukee, WI); 12-crown-4 and triglyme were degassed before use but were not subjected to any purification procedure.

Reactions Under Cold-Plasma Conditions

Selection of Starting Compounds

It has been suggested that molecular structures play a significant role in plasma-induced molecular fragmentation processes. By analyzing the molecular fragmentation mechanisms under various electron-energy mass spectroscopy (MS) conditions it was shown that the electron-energy level does not dramatically influence the relative ratios of the ion-molecular fragments in a large energy range. It was also shown that there is a strong similarity between the MS-electron and plasma-induced dissociation processes, even though these processes are not identical.[11] This behavior opens up possibilities for selecting those starting components that result in the formation of a predominant fragment that will be the main building block of the desired macromolecular structures.

The gas chromatography (GC)–MS fragmentation patterns of both 12-crown-4 and triglyme showed that $–CH_2—CH_2—O–$ was the predominant unit generated as a result of MS-electron–induced fragmentation. Recent investigations carried out in the area of *in situ* MS evaluation of RF–plasma-induced fragmentation of a number of organic compounds (e.g., isopropyl alcohol, dioxane) substantiate the suggestion that the two fragmentation mechanisms are similar.[26] Accordingly, both 12-crown-4 and triglyme were selected as precursors for the deposition of PEG-like structures.

Table I Summary of Plasma Treatments Used to Modify the Stainless Steel Surface

Sample	Surface Modification
Unmodified	Clean sample; no surface modification
O_2	Oxygen–plasma; 15 min, continuous wave, 25°C
12-Crown-4	12-Crown-4–plasma; 30 min, pulsed, 30% duty cycle, 120°C
O_2/12-Crown-4	Oxygen–plasma followed by 12-crown-4–plasma
Triglyme	Triglyme–plasma; 30 min, pulsed, 30% duty cycle, 120°C
O_2/triglyme	Oxygen–plasma followed by triglyme–plasma

Plasma Treatments

All plasma treatments were carried out in a capacitively coupled, parallel plate (20-cm diameter disk-shape electrodes with a 3-cm gap between electrodes; the lower sample-holder electrode was grounded and the upper electrode was connected to the RF power supply) cold-plasma reactor provided with heating capabilities of the monomer reservoir and reaction chamber, as previously described.[27] Each experiment was preceded by a reactor-cleaning procedure involving the following operations: wet chemical decontamination (water and acetone) of the reaction chamber; evacuation and purging of SS, vapor, and gas supply lines with oxygen; and exposure of the reaction chamber to a 30-min oxygen–plasma environment (RF-power, 250–300 W; pressure, 27 Pa; oxygen flow rate, 6 sccm). Substrates (sets of 25 SS chips) were located symmetrically on the grounded electrode and coated directly under 12-crown-4– and triglyme–plasma environments, and also after a 15-min oxygen–plasma exposure (Table I). During the plasma-coating processes the vapor-feed reservoir, SS, and vapor and gas-supply lines were thermostated at 120°C both to ensure a steady flow of the vapors and to avoid undesired condensation in the reaction chamber. Oxygen–plasma treatments were performed at a reactor temperature of 25°C.

In a typical experiment, SS samples were placed on the lower electrode and the reactor was evacuated to base pressure level. The preselected oxygen, 12-crown-4 or triglyme pressure was established, and the plasma was ignited and sustained at the selected power level, for a predetermined period of time. The following external plasma parameter space was employed for the deposition of PEG-type structures: oxygen pressure in the presence of plasma, 27 Pa; triglyme pressure in the presence of plasma, 40–45 Pa; 12-crown-4 pressure in the presence of plasma, 27–30 Pa; RF-power dissipated to the electrodes, 250 W (CW/O_2), 100 W (pulsed/triglyme), and 100 W (pulsed/12-crown-4); RF-frequency, 13.56 MHz; pulsed plasma duty cycle, 30%; pulsed plasma period, 500 μs; treatment time, 15 min (O_2), 30 min (triglyme and 12-crown-4).

At the end of the plasma reactions, the samples were aseptically removed from the reactor and stored in clean, sterile petri dishes until analytical evaluations were initiated.

Bacterial Attachment and Biofilm Formation

Unmodified and plasma-modified SS were subjected to bacterial attachment and biofilm development experiments. Three organisms were used: *Salmonella typhimurium,* a common food-borne pathogen; *Staphylococcus epidermidis,* a bacterium that causes biomaterial infection; and *Pseudomonas fluorescens,* a food spoilage bacterium. Organisms were grown individually for 12–18 h in trypticase soy broth (TSB) (BBL Microbiology Systems/ Becton Dickinson, Cockeysville, MD) at 30°C, diluted if necessary to obtain equal densities, and then combined. A portion of the combined culture (100 μL) was transferred to flasks containing 50 mL extracellular polysaccharide (EPS) medium and the SS chips and incubated at 27°C with constant agitation (100 rpm). The EPS medium was adapted from that described by LeChevallier et al.[28] and was composed of 7.0 g of K_2HPO_4, 3.0 g of KH_2PO_4, 0.1 g of $MgSO_4 \cdot 7H_2O$, 0.01 g of $CaCl_2$, 0.001 g $FeSO_4$, 0.1 g NaCl, 1.0 g glucose, and 125 mg yeast extract (Difco Laboratories, Detroit, MI), per 1 L of deionized water. The initial inoculum level was 10^4 colony-forming units (CFU)/mL.

After 1-h bacterial attachment or 1-day biofilm formation, the SS chips were removed from the flasks and rinsed twice in 10 m*M* phosphate-buffered saline (PBS, pH 7.2) and once in distilled

water. The chips were vortexed for 30 s in 5 mL PBS containing glass beads to detach biofilm cells from the surfaces. The number of attached cells was evaluated by plating onto tryptic soy agar (Difco) plates. The plates were incubated at 30°C for 48 h and the numbers of CFUs developed were counted.

Statistical analysis of the data was performed using the Minitab statistical software package. A two-sample *t*-test was used with a confidence interval of 90%. Differences between the numbers of CFUs on modified and unmodified samples were considered statistically significant at $p < 0.05$.

Surface Analyses

Survey and high-resolution (HR) ESCA evaluations of unmodified and plasma-coated SS and biofilms that developed on these surfaces were performed using a Perkin–Elmer Physical Electronics 5400 Small Area Spectrometer (Mg source, 300 W, 15 kV, 45° take-off angle; Perkin–Elmer, Palo Alto, CA). Generally, acquisition times of less than 2 min were employed to avoid X-ray–induced damage of the sample. However, increased times (3–4 min) were used for acquisition of P and N data to avoid a noisy background of the spectra.

Water contact angle analysis for evaluating relative hydrophilic or hydrophobic characteristics was carried out with a Rame Hart contact angle goniometer (Mountain Lakes, NJ).

The presence of plasma-deposited macromolecular layers and changes in surface topography or surface roughness were assessed by AFM using a Digital Instruments Nanoscopy III microscope (scan area, 14 μm^2; number of scans, 512; scan rate, 1.9 Hz; silicon nitride Nanoprobe, ™SPM tips, type NP; Digital Instruments, Santa Barbara, CA). The roughness values were defined and calculated according to the following formulas, definitions, and criteria.[29] *Z*-range represents the difference between the highest and the lowest points within the given area. R_{ms} (R_q) stands for the standard deviation of *Z* values within the given area and is expressed as

$$R_q = \sqrt{\frac{\sum (Z_i - Z_{\text{ave}})^2}{N}} \qquad (1)$$

where Z_{ave} (mean) is the average of the *Z* values within the given area; Z_i is the current *Z* value, and *N* is the number of points within the given area. R_a (mean roughness) is the mean value of the surface relative to the center plane and can be evaluated using the following equation:

$$R_a = \frac{1}{L_x L_y} \int_0^{L_y} \int_0^{L_x} f(x, y)\, dx\, dy \qquad (2)$$

where $f(x, y)$ is the surface relative to the center plane and L_x and L_y are the dimensions of the surface.

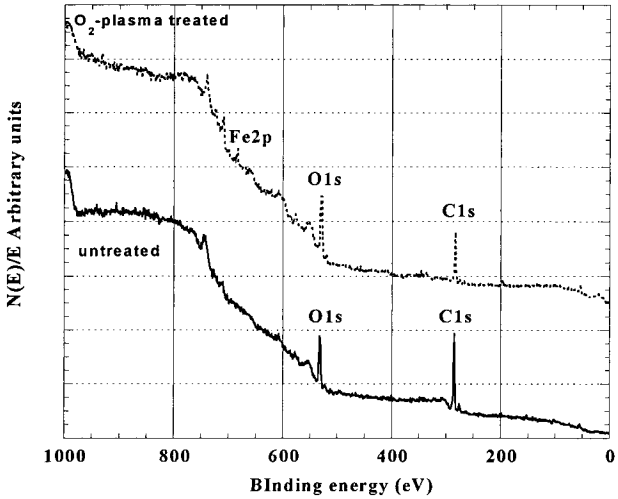

Figure 1 Survey ESCA of unmodified (solid line) and oxygen–plasma-treated (dotted line) stainless steel.

RESULTS AND DISCUSSION

Surface Chemistry and Characteristics of Unmodified and Plasma-Coated SS

ESCA

The percentage composition of 304 stainless steel is 0.08% carbon, 2% manganese, 1% silicon, 18–20% chromium, 8–12% nickel, 0.04% phosphorus, and 0.03% sulfur.[30] However, survey ESCA data indicated the presence of a significant amount of environmental contamination–origin carbon (C1s, 61%) and oxygen (O1s, 30%) on the surfaces of clean stainless steel substrates (Figs. 1 and 2) and relatively low iron (Fe2p, 3%) and chromium (Cr2p, 3%) surface atomic concentrations. HR C1s ESCA of unmodified SS surfaces [Fig. 3(A)] showed the presence of oxidized, hydrocarbon-like structures. In addition to the dominant C—C/C—H binding energy

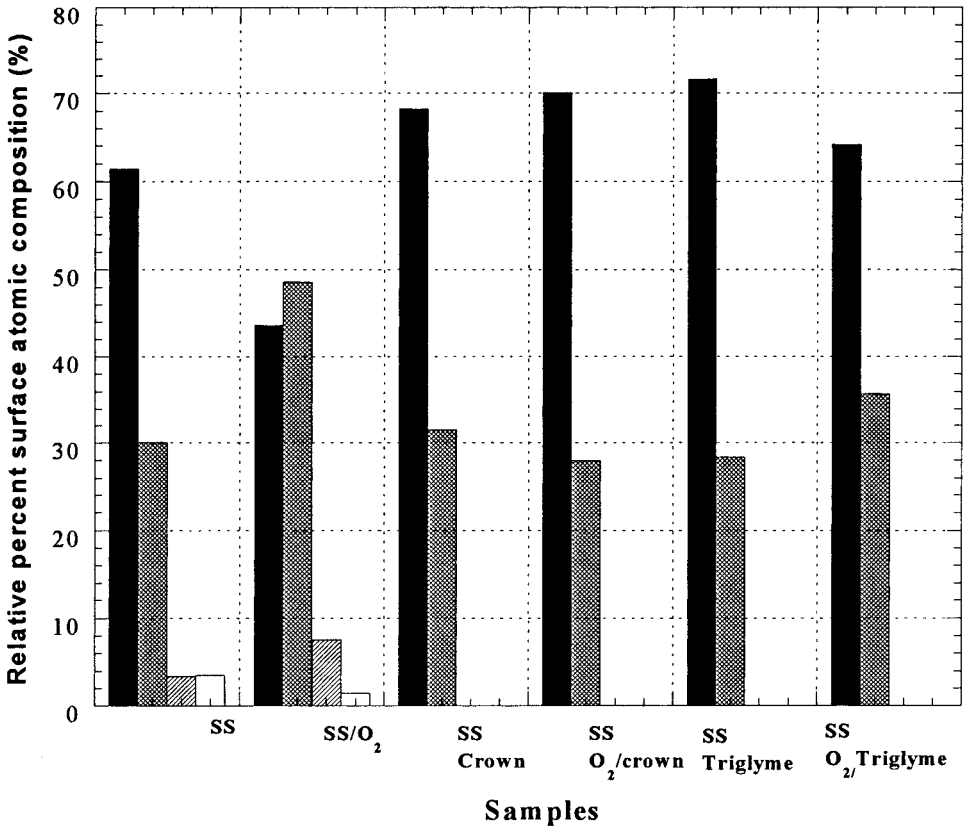

Figure 2 Relative percentage surface atomic composition of unmodified and plasma-modified stainless steel. Solid bars, C1s; hatched bars, O1s; diagonally shaded bars, Fe2p; empty bars, Cr2p.

peak, low surface area C- and O-based peaks were identified (C—O, O—C═O).

Oxygen–plasma treatment significantly modified the SS surface structure and characteristics. The relative surface atomic composition showed a 20% decrease in C1s and a slight increase in the relative surface iron concentration (Fe2p = 8%) (Fig. 1). The significant increase in the O/C ratio (1.09; O1s = 48%, C1s = 44%) relative to that of the unmodified surface (0.48; O1s = 30%, C1s = 62%) (Fig. 2), the appearance of C═O functionalities, and a higher relative percentage of O—C═O (Table II) demonstrated that an intense oxidation process rather than ablation had occurred. The simultaneous development of plasma-induced oxidation and etching reactions rendered the formation of very thin (400–600 nm, estimated based on the interference pattern) oxidized layers, which explains the high noise level in the HR ESCA spectrum [Fig. 3(B)]. These layers can contain free-radical– or surface-charge–bearing active species that could play an important role in mediating the covalent attachment of PEG-like plasma-generated macromolecular structures.

Survey ESCA data collected from all 12-crown-4– and triglyme–plasma-treated samples with or without initial oxygen–plasma treatment (Fig. 4 and Table II) showed the presence of surface-layer structures composed of only oxygen and carbon atoms. Their relative surface carbon and oxygen atomic compositions were 64 to 72% (C1s) and 28 to 32% (O1s), which corresponded to O/C ratios of 0.39 to 0.55. The theoretical O/C ratio for PEG is 0.50, and the HR C1s ESCA exhibits a unimodal symmetrical C—O (286.4 eV) binding energy peak attributed to the presence of $-(CH_2—CH_2—O)_n-$ repeating units.

However, a comparison of relative surface atomic concentrations does not necessarily indicate the presence of identical functionalities. Analysis of nonequivalent C1s functionalities is required to evaluate the nature and relative ratios of carbon-based linkages of plasma-generated layers. HR C1s ESCA data indicated that the

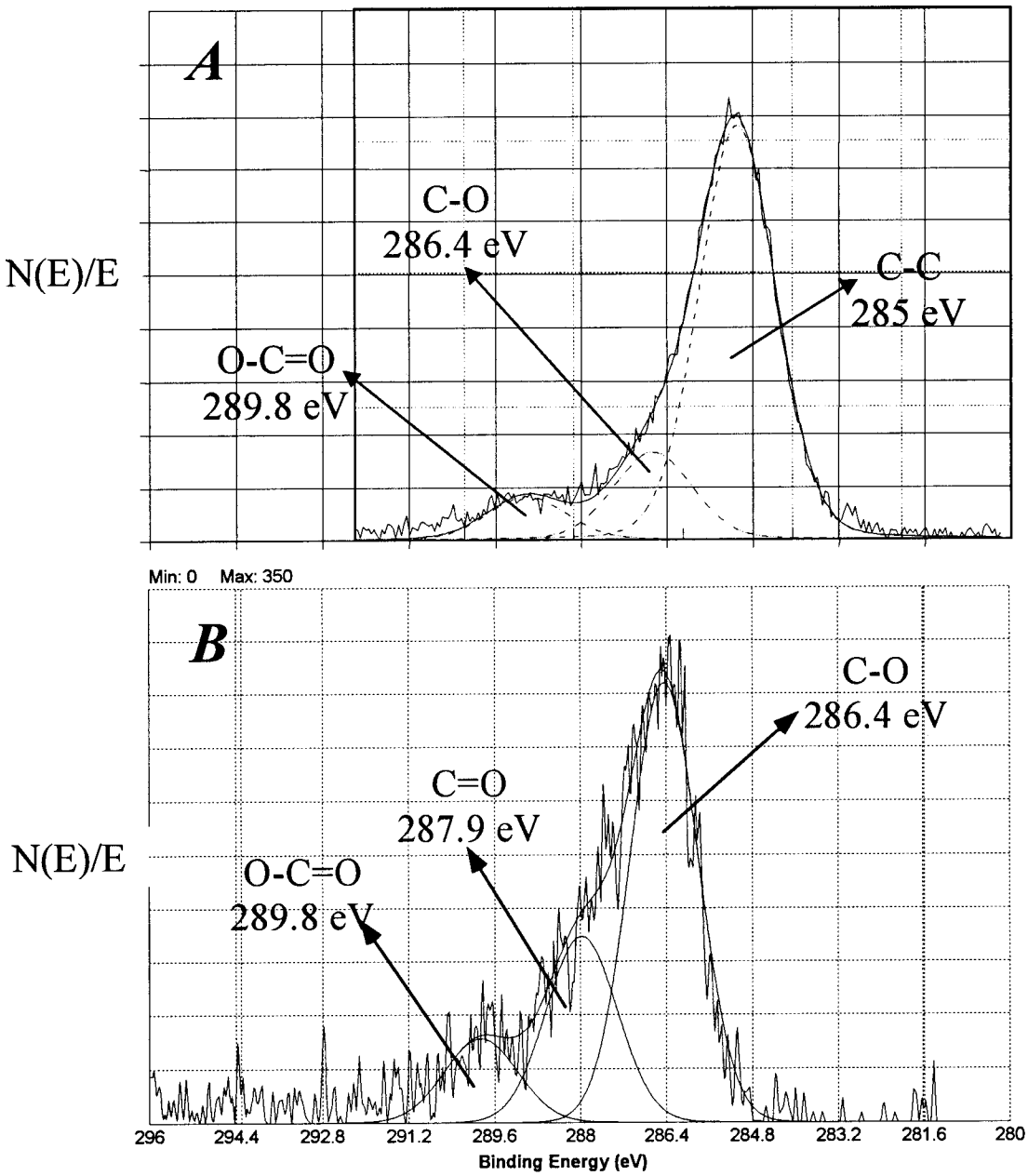

Figure 3 High-resolution C1s ESCA of (A) unmodified and (B) oxygen–plasma-treated stainless steel.

C—O peak had the highest surface area in the C1s region of all plasma-modified SS surfaces.

The 12-crown-4–plasma-coated SS obtained in this study shows the presence of a low surface area C—C binding energy peak in addition to the dominant peak area C—O linkage [Fig. 5(A)]. This indicates that dehydrogenation processes also accompanied the plasma-enhanced ring-opening mechanism of crown–ether molecules. It is noteworthy that the crown-4–plasma-treated SS contained the highest relative percentage of C—O functionality, and was the only sample that did not contain O—C═O (Table II). The presence of hydrogen atoms in the plasma might also be responsible for the absence of O—C═O functionalities as a result of the development of gas-phase and surface-mediated hydrogenation mechanisms.

C—C linkages were not detected in the surface layers of oxygen/12-crown-4–plasma-treated SS

Table II Relative Percentage Nonequivalent Carbon Functionalities of Unmodified and Plasma-Modified Stainless Steel

	Relative Percentage				
Sample	C—C	C—O	C═O	O—C═O	O—CO—O
Unmodified	73.5	18.0	0	8.4	0
O_2	0	60.0	26.8	12.5	0
12-Crown-4	25.4	63.2	4.8	0	0
O_2/12-Crown-4	0	58.3	20.2	8.4	13.1
Triglyme	0	50.9	37.4	11.6	0
O_2/triglyme	0	57.0	20.0	19.2	3.6
Theoretical PEG/PEO	0	100	0	0	0

samples [Fig. 5(B)]. However, the resulting macromolecular layers contained significant amounts of C═O, O—C═O, and O—CO—O functionalities. These findings support our initial hypothesis that the formation of oxygen–plasma-generated structures and active species (e.g., free-radical sites) rendered a surface recombination mechanism of 12-crown-4–origin molecular fragments different from that developed on a nonoxidized surface. It also should be noted that free-radical species trapped in the nascent macromolecular networks could initiate intense *ex situ* oxidation reactions under open laboratory conditions.

HR ESCA results obtained with triglyme– and oxygen/triglyme–plasma-treated SS are shown in Figure 6. Triglyme-treated samples exhibited the lowest O/C ratio (0.39; O1s = 28%, C1s = 72%), and unlike the 12-crown-4–treated surfaces, the presence of C—C linkages was negligible. In the

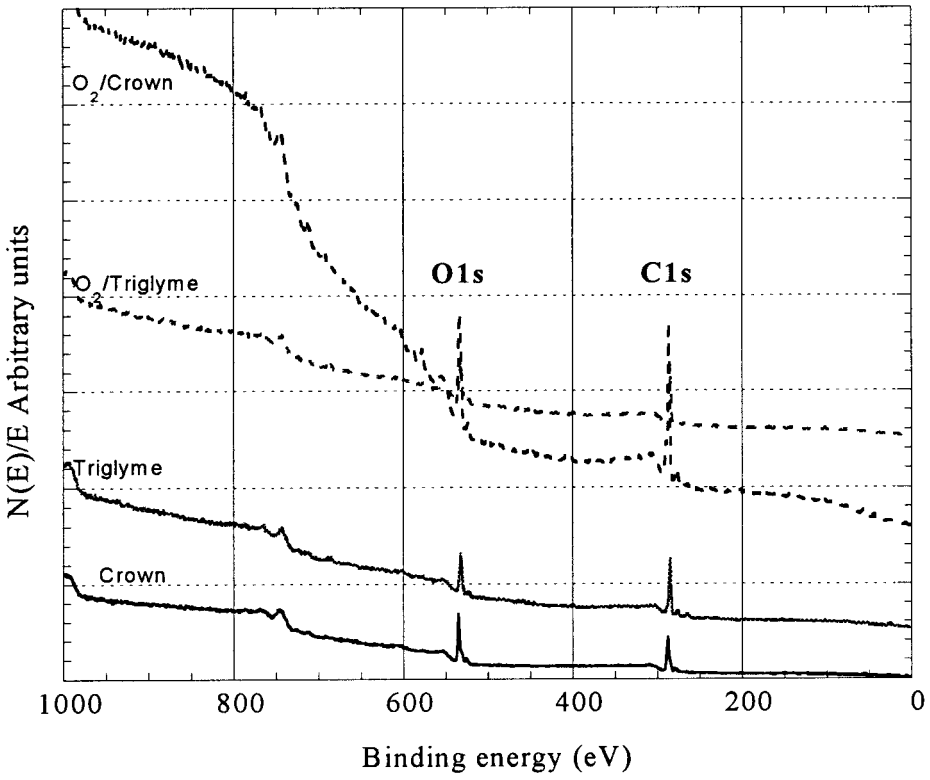

Figure 4 Survey ESCA of stainless steel plasma-treated with 12-crown-4, oxygen/12-crown-4, triglyme, or oxygen/triglyme.

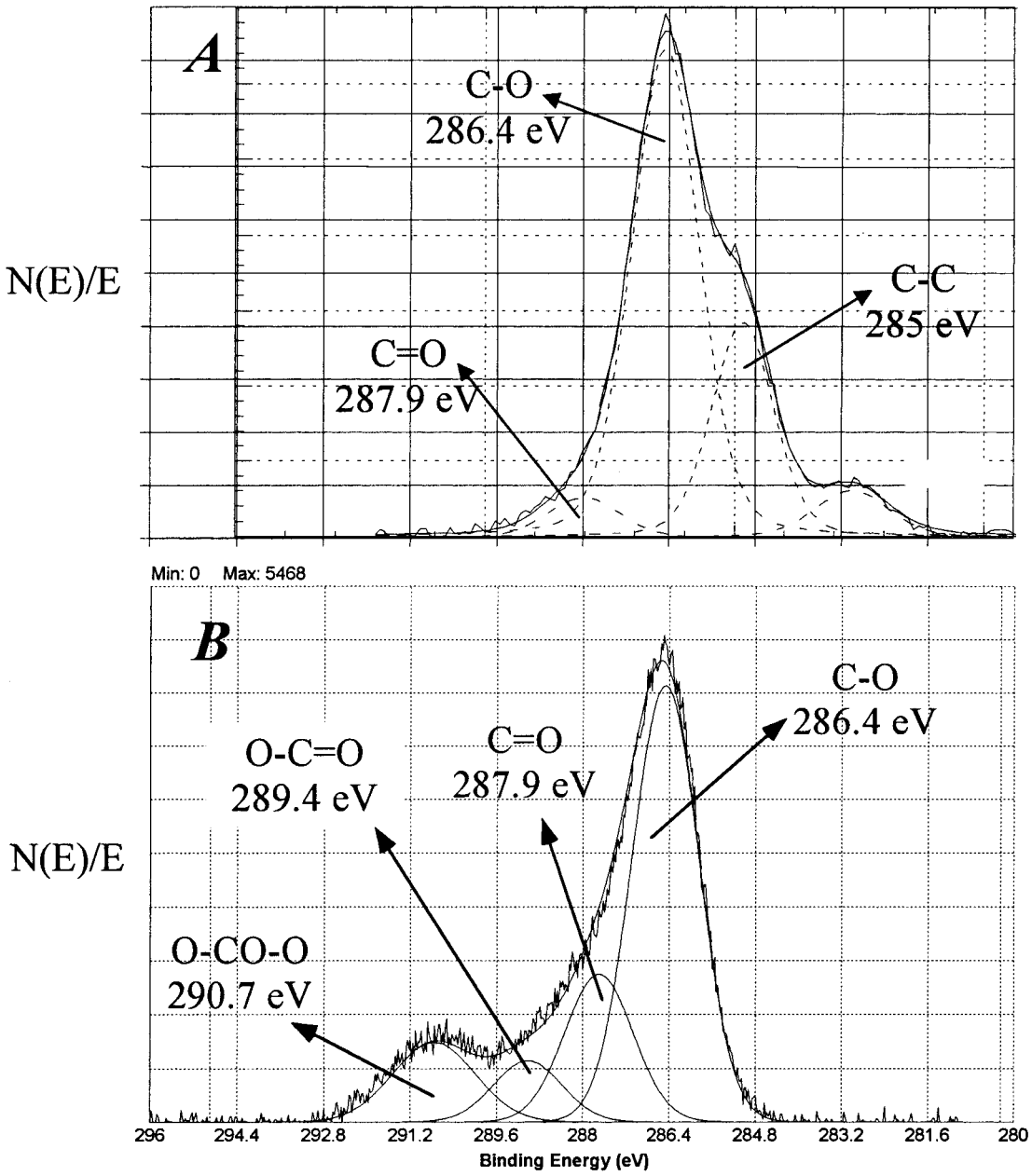

Figure 5 High-resolution C1s ESCA of (A) 12-crown-4–plasma-coated and (B) oxygen/12-crown-4–plasma-coated stainless steel.

case of oxygen/triglyme-treated SS, the O/C ratio (0.55; O1s = 35%, C1s = 64%) was higher, and similar to the oxygen/crown-4–treated substrates, O—CO—O– functionalities were also present in the structure of the deposited layers (Table II).

Contact Angle

Figure 7 shows contact angle data for unmodified and plasma-modified substrates. A contact angle of 86° associated with the unmodified SS might be related to the presence of oxidized hydrocarbon–type structures, as evidenced by HR ESCA. Our results are in agreement with reported values of 85–86° for cleaned SS type 304.[31] As expected, significantly lower contact angles were recorded in the case of oxygen–plasma-treated samples. The formation of polar functional groups (C—O, C═O) as a result of the oxygen–plasma exposure of SS could be responsible for the generation of

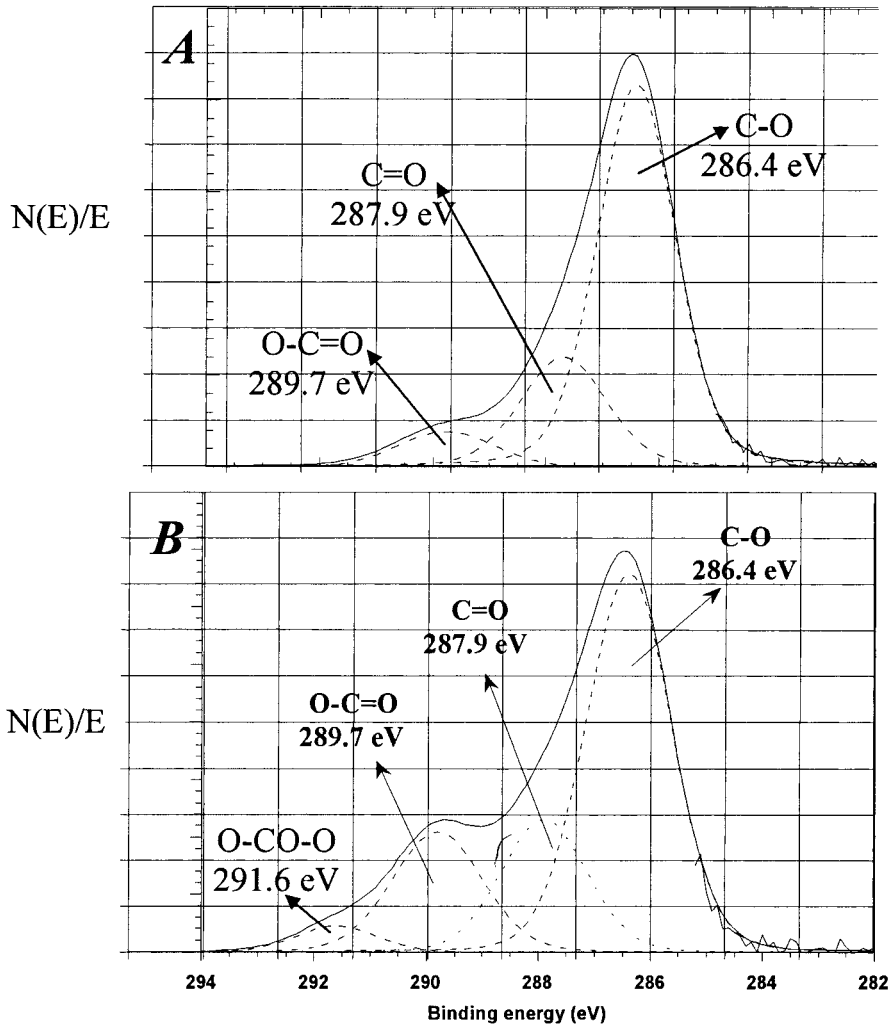

Figure 6 High-resolution C1s ESCA of (A) triglyme–plasma-coated and (B) oxygen/triglyme–plasma-coated stainless steel.

the lower contact angles. All plasma-modified samples exhibited fewer hydrophobic surfaces than did the unmodified sample. The lowest contact angles (i.e., the most hydrophilic surfaces) were recorded in the case of the oxygen/triglyme–plasma-coated SS.

Biofilms that developed on unmodified and plasma-modified surfaces had lower contact angles (more hydrophilic) than their respective surfaces without biofilm. The only exception was the oxygen–plasma-modified surface, which had the highest contact angle of 63°.

AFM

A typical AFM image of an unmodified SS surface is shown in Figure 8(A). The grooves exhibited by the image are characteristic of the No. 4 finish of the SS surface. Figure 8(B) shows the SS surface topography after the development of a bacterial biofilm. The surface was partially covered by the biofilm. Nonuniform coverage of a surface is typical in biofilm development. AFM images (acquired at a magnification of 12.5 μm) of 12-crown-4– and triglyme–plasma-coated SS appeared similar (not shown). The surface roughness values of 12-crown-4–coated (R_{ms} = 191.3 nm; R_a = 157.9 nm) and triglyme-coated (R_{ms} = 123.6 nm; R_a = 98.7 nm) samples were lower compared to those of the unmodified SS samples (R_{ms} = 245.0 nm; R_a = 195.3 nm). Deposition of PEG-like layers on SS apparently reduced the roughness of the surface.

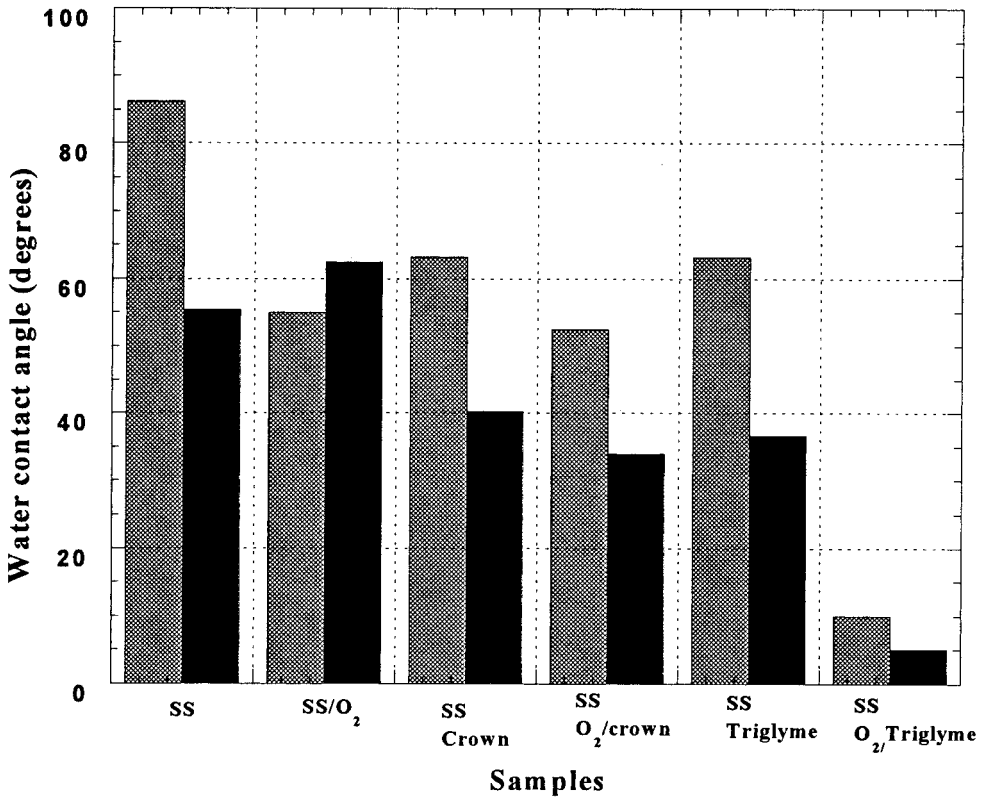

Figure 7 Water contact angles of unmodified and plasma-modified stainless steel (hatched bars) and biofilms developed on the surfaces (solid bars).

Bacterial Attachment and Biofilm Formation and Surface Characteristics

ESCA

ESCA has been used to study the cell surface composition of a wide range of bacteria. Data were compiled in a recent review for over 210 strains. Generally, bacterial cells were washed, freeze-dried, and packed into the cell holder for ESCA.[32] In our study, ESCA was performed directly on the dried biofilm, thus minimizing some of the artifacts that could be caused by sample preparation. Biofilms that developed on unmodified, oxygen–plasma, and 12-crown-4– and triglyme–plasma-modified SS were evaluated by ESCA.

Cell surface composition can be compared by calculating the relative ratios of O/C (reflecting the presence of proteins and polysaccharides), N/C (proteins), and P/C (lipopolysaccharides, lipoproteins, and phospholipids). Whereas a mixed culture was used for attachment and biofilm formation, visual observation of colony morphology on agar plates showed that at least 90% of the bacteria recovered from biofilms were typical for *S. typhimurium*. ESCA was used to identify lipopolysaccharides and proteins as the main cell surface components of two strains of *S. typhimurium*.[33] We observed that the biofilm cell surface composition varied and was dependent on the plasma treatment applied to SS (Table III). The ratios of relative percentage atomic composition for biofilms on 12-crown-4– and triglyme–plasma-modified surfaces were similar. The N/C ratios were slightly lower, whereas the P/C ratios were 2.5- to threefold less than the respective ratios from an unmodified surface. This suggested that the surface compositions of the biofilms were different. Biofilms on oxygen–plasma-treated SS had a distinctly different composition, with the highest O/C, N/C, and P/C ratios among the four biofilm samples. It has been shown that increasing hydrophobicity could be directly related to increasing N/C ratios,[32] which would account for, at least partially, the rank order of the biofilm contact angle results (Fig. 7).

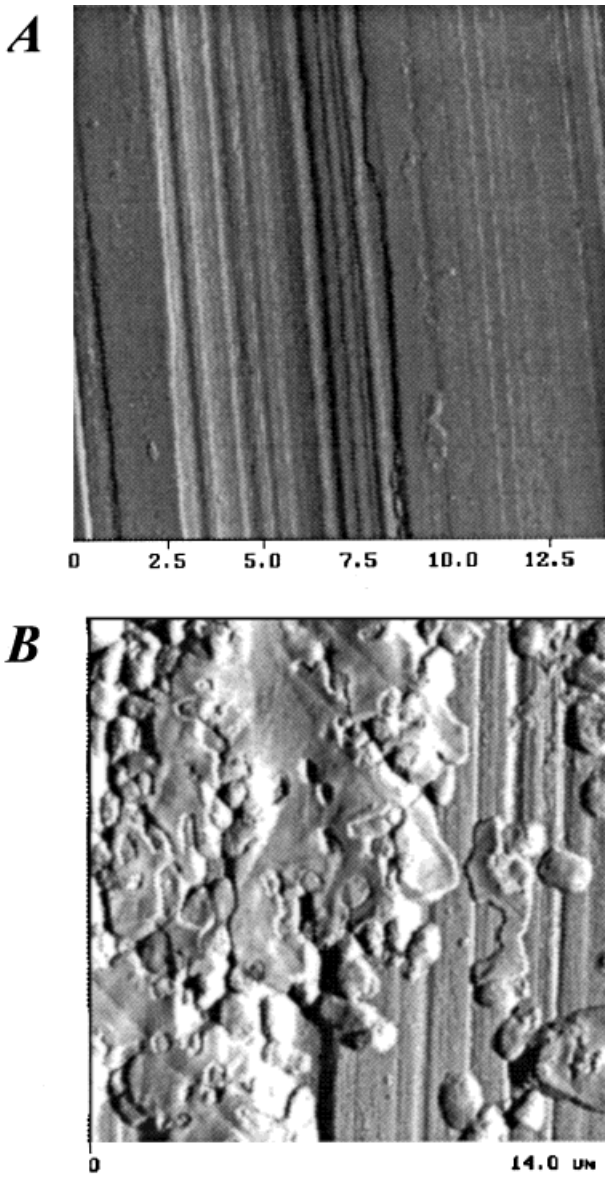

Figure 8 AFM image of (A) unmodified stainless steel and (B) 1-day biofilm developed on unmodified stainless steel.

Bacteria Attachment and Biofilm Formation

The levels of bacterial attachment and biofilm formation on unmodified and plasma-modified SS are presented in Tables IV and V. Both bacterial attachment and biofilm formation were increased as a result of the oxygen–plasma treatment of SS (Table IV). Surface oxidation reactions and an intense etching that accompany the oxygen–plasma process usually result in an increased surface roughness that might enhance bacterial adhesion. It has been shown in some studies that even a small increase in surface roughness can influence the adhesion of microorganisms.[34] Alternatively, oxygen–plasma can increase the oxidized layer of the surface. In addition to the presence of chromium, the relative surface composition of iron increased to 8% after oxygen–plasma treatment of SS. It has been demonstrated that there was an increase in attachment of streptococci to type 304 SS surfaces with oxide coatings compared to those with the oxide layers removed.[31]

Deposition of PEG-like structures on SS, on the other hand, had the opposite and desired effect. Compared to unmodified SS, bacterial attachment and biofilm formation were decreased by 56.5 and 72.2%, respectively, on 12-crown-4–plasma-coated SS, and by 82.2 and 94.0%, respectively, on triglyme-modified samples (Table V). Our results with the triglyme-modified SS are in agreement with those reported for triglyme-

Table III Bacterial Cell Surface Composition of 1-Day Biofilms on Unmodified and Plasma-Modified Stainless Steel

	Ratios of Relative Percentage of Atomic Composition		
Surface	O/C	N/C	P/C
Unmodified SS	0.45	0.05	0.01
O_2 plasma	0.60	0.07	0.02
12-Crown-4–plasma	0.49	0.04	0.003
Triglyme–plasma	0.49	0.03	0.004

Table IV Effect of 15-Min Oxygen–Plasma Treatment of Stainless Steel on 1-h Attachment and 1-day Biofilm Formation by a Mixed Culture of *Salmonella typhimurium*, *Staphylococcus epidermidis*, and *Pseudomonas fluorescens*

	1-h Attachment		1-day Biofilm	
Sample	Log CFU/cm^2	% Change[a]	Log CFU/cm^2	% Change
Unmodified	4.24	—	8.93	—
O_2	4.74	215% inc.[b]	9.10	47.9% inc.

[a] Percentage change compared to unmodified sample (inc. = increase; dec. = decrease).
[b] Denotes statistically significant difference.

Table V Effect of Different Plasma Treatments of Stainless Steel on 1-h Attachment and 1-day Biofilm Formation by a Mixed Culture of *Salmonella typhimurium, Staphylococcus epidermidis,* and *Pseudomonas fluorescens*

	1-h Attachment		1-Day Biofilm	
Sample	Log CFU/cm^2	% Change	Log CFU/cm^2	% Change
Unmodified	5.45	—	8.05	—
12-Crown-4	5.08	56.5% dec.[b]	7.49	72.2% dec.[b]
O_2/12-Crown-4	5.34	21% dec.	8.06	3.3% inc.
Unmodified	5.14	—	8.20	—
Triglyme	4.39	82.2% dec.[b]	6.98	94.0% dec.[b]
O_2/triglyme	5.44	101% inc.[b]	8.73	240% inc.[b]

[a] Percentage change compared to unmodified sample (inc. = increase; dec. = decrease).
[b] Denotes statistically significant difference.

coated PEU, which reduced attachment and biofilm formation by *P. aeruginosa.*[21]

Bacterial attachment was decreased by 21% in the case of oxygen/12-crown-4–plasma-modified surfaces, whereas the level of biofilm formation was essentially the same as that on unmodified SS. The oxygen–plasma treatment of SS had an even more detrimental effect on the antifouling characteristics of triglyme–plasma-coated substrates. A significant increase in bacterial attachment and biofilm formation was observed on oxygen/triglyme–plasma-modified SS samples (Table V).

It is possible that the surface layers generated as a result of oxygen–plasma exposure of hydrocarbon-type structures present on SS rendered the development of different recombination mechanisms of 12-crown-4– and triglyme–plasma species compared to that of nonoxidized surfaces, resulting in different surface characteristics. A more crosslinked structure, for instance, might significantly reduce the mobility of PEG-type molecular chains and diminish the antifouling characteristics.

Overall, the levels of bacterial attachment and biofilm formation could not be related to surface contact angle or the relative percentage of C—O functionalities. However, there was a correlation between the O/C ratio and bacterial attachment. Oxygen–plasma-treated SS, which had the highest O/C ratio (1.09), had the highest number of attached bacteria; triglyme–plasma-treated SS had the lowest O/C ratio (0.39) and the least number of attached bacteria.

Stability of the biofilms was evaluated by washing the samples in PBS for 30 min with agitation. The number of biofilm bacteria decreased on all samples after washing. Even though the number on oxygen–plasma-treated SS was higher than the control, the number decreased by 23.5% more than that on the unmodified SS after washing. The decrease was also higher with both 12-crown-4– and triglyme–plasma-coated samples (by 64.4 and 75.0%, respectively). These results indicate that biofilm bacteria are less adhesive on plasma-coated SS. Consequently, if these plasma treatments are applied to surfaces used in food processing, any biofilms that develop may be more easily removed by routine cleaning procedures.

CONCLUSIONS

It has been observed that 12-crown-4– and triglyme–plasma environments are suitable for the deposition of PEG-like structures on SS surfaces. Significantly reduced bacterial attachment and biofilm formation were achieved on 12-crown-4– and triglyme–plasma-coated surfaces in the presence of a mixed culture of *S. typhimurium, S. epidermidis,* and *P. fluorescens.* Biofilms that developed on these and oxygen–plasma-coated surfaces were less stable and easier to remove than those on uncoated surfaces. The higher level of bacterial attachment and biofilm formation on oxygen–plasma-treated and, subsequently, 12-crown-4– and triglyme–plasma-coated surfaces can probably be explained by the development of a different recombination mechanism of plasma species in the presence of an oxidized/crosslinked surface structure. The RF–plasma approach can

have potential applications in depositing antifouling layers on a multitude of materials, such as those used in food-processing equipment, medical implants, and catheters.

REFERENCES

1. Characklis, W. G. in Biofilms; Characklis, W. G.; Marshall, K. C., Eds.; Wiley: New York, 1990; pp. 195–231.
2. Harris, J. M., Zalipski, S., Eds. Poly(ethylene glycol): Chemistry and Biological Applications; ACS Symposium Series 680; American Chemical Society: Washington, DC, 1997.
3. Gombotz, W. R.; Guanghui, W.; Horbett, T. A.; Hoffman, A. S. in Poly(ethylene glycol) Chemistry: Biotechnical and Biomedical Applications; Harris, J. M., Ed.; Plenum Press: New York, 1992; pp. 47–261.
4. Osterberg, E.; Bergstrom, K.; Holmberg, K.; Schuman, T. P.; Riggs, J. A.; Burn, L.; Alstine, V.; Harris, J. M. J Biomed Mater Res 1995, 29, 741.
5. Lee, J. H.; Kopecek, J.; Andrade, J. D. J Biomed Mater Res 1989, 23, 351.
6. Holmberg, K.; Bergstrom, K.; Brink, C.; Osterberg, E.; Tiberg, F.; Harris, M. in Contact Angle Wettability and Adhesion; Mittal, K. L., Ed.; VSP, Utrecht, The Netherlands 1993; pp. 813–927.
7. Ista, L. K.; Fan, H.; Baca, O.; Lopez, G. P. FEMS Microbiol Lett 1996, 142, 59.
8. Amiji, M.; Park, K. J Biomater Sci Polym Ed 1993, 4, 217.
9. Park, K. D.; Kim, J. S.; Han, D. K.; Kim, Y. H.; Lee, E. H. B.; Suh, H.; Choi, K. S. Biomaterials 1998, 19, 851.
10. Shi, F. F. Surf Coat Technol 1996, 82, 1.
11. Denes, F. TRIP 1997, 5, 23.
12. Sarmadi, A. M.; Denes, A. R.; Denes, F. Text Chem Color J 1996, 28, 17.
13. Hsiue, G.-H.; Lee, S.-D.; Chang, P. C.-T.; Kao, C.-Y. J Biomed Mater Res 1998, 42, 134.
14. Tang, L.; Wu, Y.; Timmons, R. B. J Biomed Mater Res 1998, 42, 156.
15. Ratner, B. D. J Biomater Sci Polym Ed 1992, 4, 3.
16. Ratner, B. D. Biosens Bioelectron 1995, 10, 797.
17. Lopez, G. P.; Ratner, B. D.; Tidwell, C. D.; Haycox, C. L.; Rapoza, R. J.; Horbett, T. A. J Biomed Mater Res 1992, 26, 415.
18. Johnston, E. E.; Ratner, B. D. in Surface Modification of Polymeric Biomaterials; Ratner, B. D.; Castner, D. G., Eds.; Plenum Press: New York, 1996; pp. 35–44.
19. Rad, A. Y.; Ayhan, H.; Piskin, E. J Biomed Mater Res 1998, 41, 349.
20. Morra, M.; Cassinelli, C. J Biomed Mater Res 1996, 31, 149.
21. Hendricks, S. K.; Kwok, C.; Shen, M.; Horbett, T. A.; Ratner, B. D.; Bryers, J. D. J Biomed Mater Res 2000, 50, 160.
22. Rinsch, C. L.; Chen, X.; Panchalingan, V.; Eberhardt, R. C.; Wang, J.-H.; Timmons, R. B. Langmuir 1996, 12, 2995.
23. Chen, X.; Rajewhar, K.; Timmons, R. B.; Chen, J.-J.; Chyan, M. R. Chem Mater 1996, 8, 1067.
24. Han, L. M.; Timmons, R. B.; Bogdal, D.; Pielichowski, J. Chem Mater 1998, 10, 1422.
25. Panchalingam, V.; Chen, X.; Huo, H.-H.; Savage, C. R.; Timmons, R. B.; Eberhart, R. C. ASAIO J 1993, 30, 305.
26. Shamamian, V.; Manolache, S.; Denes, F. J Appl Phys to appear.
27. Denes, F. J Appl Polym Sci 1999, 71, 1627.
28. LeChevallier, M. W.; Cawthon, C. D.; Lee, R. G. Appl Environ Microbiol 1988, 54, 649.
29. Digital Instruments Nanoscope III Scanning Probe Microscope User's Manual; Digital Instruments: Santa Barbara, CA.
30. West, R. C., Ed. Handbook of Chemistry and Physics; CRC Press: Cleveland, OH, 1976; p. F-156.
31. Flint, S. H.; Brooks, J. D.; Bremer, P. J. J Food Eng 2000, 43, 235.
32. van der Mei, H. C.; de Vries, J.; Busscher, H. J. Surf Sci Rep 2000, 39, 1.
33. Magnusson, K. E.; Johansson, L. Stud Biophys 1977, 66, 145.
34. Taylor, R. L.; Verran, J.; Lees, G. C.; Ward, A. J. P. J Mater Sci Mater Med 1998, 9, 17.